

Supporting Information for “Thermodynamic and dynamic controls on changes in the zonally anomalous hydrological cycle”

Robert C. Wills^{1,2}, Michael P. Byrne¹, and Tapio Schneider^{1,2}

Contents of this file

1. Table S1
2. Figures S1 to S6

Introduction

Table S1 shows a list of the 23 CMIP5 models used in this study. All 23 models that have published monthly-mean precipitation (P), evaporation (E), surface-air temperature (T_s), surface-air specific humidity (q_s), horizontal wind (\mathbf{u}), specific humidity (q), and vertical pressure velocity (ω) are considered

Fig. S1 shows the zonal-mean $P - E$ change, its approximation by the simple thermodynamic scaling (Eq. 1 in the main text), and the extent to which the thermodynamic

¹Geological Institute, ETH Zürich,
Zürich, Switzerland

²California Institute of Technology,
Pasadena, California, USA

scaling is modified by considering seasonal correlations between moisture changes and $P - E$.

Fig. S2 shows the extent to which $\delta\text{RMS}_{\text{mthermo}}$ can be estimated from the climatological stationary-eddy contribution to $P^* - E^*$ and the fractional change in surface specific humidity, where Δ_{thermo} is replaced by

$$\Delta_{\text{estimate}} = -\frac{\delta[q_s]}{[q_s]}\nabla \cdot \langle \mathbf{u}q \rangle^* \quad (1)$$

in Eq. (17) of the main text.

Fig. S3 shows the decomposition of the transient-eddy terms in Figs. 2 and 4c into synoptic (departure from monthly means) and seasonal-correlation components.

Fig. S4 and S5 show results of the analysis described in the main text for JJA and DJF respectively. Note that due to the nonlinearity of the rms operator, the annual-mean results presented in the main text differ from the average of results performed separately for each season. We have also checked the analysis for individual months. The main conclusions of the paper hold for any month or season studied.

Fig. S6 shows an illustration of the grid-scale noise present in unprocessed ω_{850} , from select CMIP5 models. This shows raw monthly-mean data, downloaded directly from the Earth System Grid. Some models (e.g., CNRM-CM5, MRI-CGCM3, etc.) have unrealistic grid-scale noise in ω_{850} . Given the importance of ω_{850} in the hydrological cycle, as outlined in this study, some effort needs to be taken to improve the vertical velocity output from CMIP5 models.

Table 1. CMIP5 models used for zonally-anomalous moisture budget analysis.

Model	Description
CCSM4	Community Climate System Model, version 4
CESM1-BGC	Community Earth System Model, version 1 (Biogeochemistry)
CESM1-CAM5	Community Earth System Model, version 1 (Community Atmosphere Model, version 5)
CNRM-CM5	Centre National de Recherches Meteorologiques Coupled Global Climate Model, version 5
CanESM2	Second Generation Canadian Earth System Model
FGOALS-g2	Flexible Global Ocean–Atmosphere–Land System Model gridpoint, version 1.0
GFDL-CM3	Geophysical Fluid Dynamics Laboratory Climate Model, version 3
GFDL-ESM2G	Geophysical Fluid Dynamics Laboratory Earth System Model with Generalized Ocean Layer Dynamics (GOLD) component
GFDL-ESM2M	Geophysical Fluid Dynamics Laboratory Earth System Model with Modular Ocean Model 4 (MOM4) component (ESM2M)
GISS-E2-H	Goddard Institute for Space Studies Model E, coupled with the HYCOM ocean model
HadGEM2-ES	Hadley Centre Global Environment Model, version 2 (Earth System)
IPSL-CM5A-LR	L’Institut Pierre-Simon Laplace Coupled Model, version 5A, coupled with NEMO, low resolution
IPSL-CM5A-MR	L’Institut Pierre-Simon Laplace Coupled Model, version 5A, coupled with NEMO, mid resolution
IPSL-CM5B-LR	L’Institut Pierre-Simon Laplace Coupled Model, version 5B, coupled with NEMO, low resolution
MIROC-ESM	Model for Interdisciplinary Research on Climate, Earth System Model
MIROC-ESM-CHEM	Model for Interdisciplinary Research on Climate, Earth System Model, Chemistry Coupled
MIROC5	Model for Interdisciplinary Research on Climate, version 5
MRI-CGCM3	Meteorological Research Institute Coupled Atmosphere–Ocean General Circulation Model, version 3
NorESM1-M	Norwegian Earth System Model, version 1 (intermediate resolution)
NorESM1-ME	Norwegian Earth System Model, version 1 (intermediate resolution), with prognostic biogeochemical cycling
bcc-csm1-1	Beijing Climate Center, Climate System Model, version 1.1
bcc-csm1-1-m	Beijing Climate Center, Climate System Model, version 1.1, moderate resolution
inmcm4	Institute of Numerical Mathematics Coupled Model, version 4.0

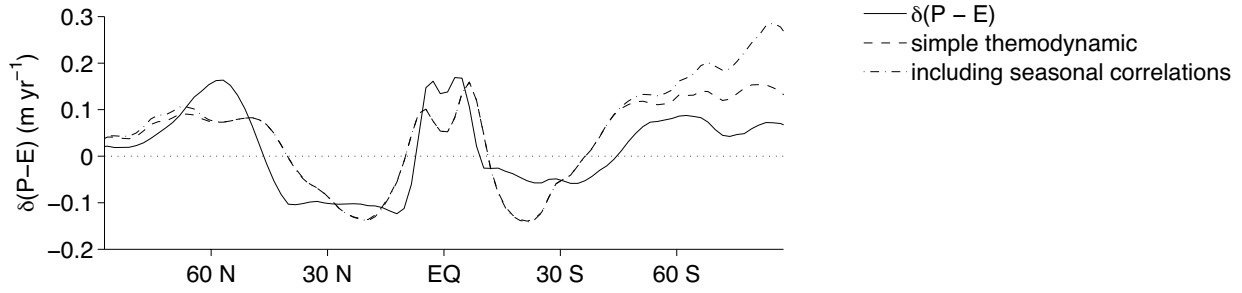


Figure S1. Zonal-mean $P - E$ change and a simple thermodynamic scaling (dashed line, Eq. 1 in the main text). If seasonal correlations between moisture changes and $P - E$ are included (dash-dotted line), the scaling significantly overestimates the change in high northern latitudes, due to strong polar amplification in winter.

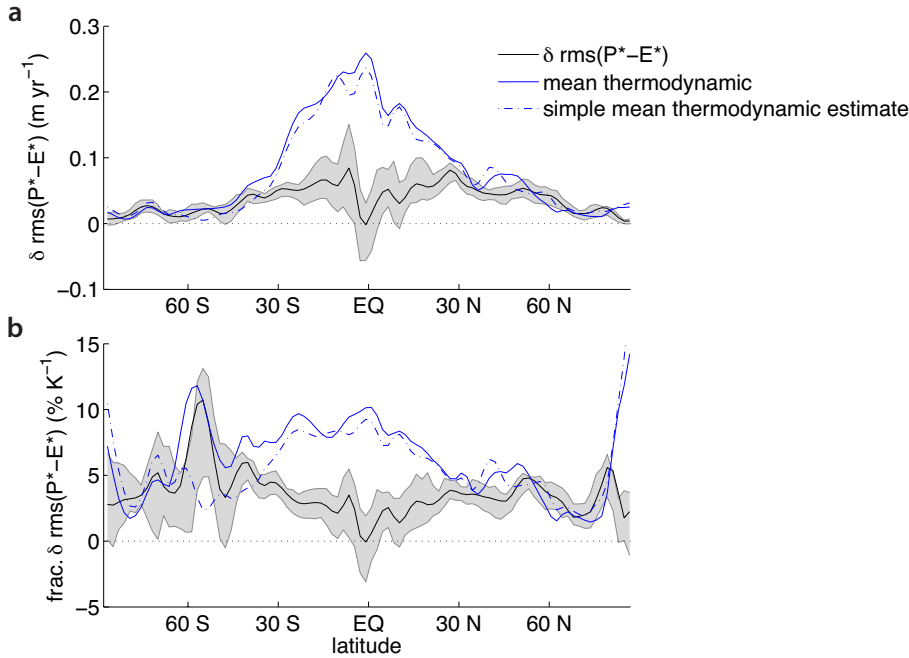


Figure S2. Full stationary-eddy thermodynamic changes in $\text{rms}(P^* - E^*)$ (solid blue lines) and an estimate based on scaling the climatological stationary-eddy moisture flux convergence by the change in surface specific humidity, $-\frac{\delta[q_s]}{[q_s]}\nabla \cdot \langle \mathbf{u}q \rangle^*$ (dashed blue lines). Subpanel a) shows absolute changes; b) shows fractional changes. The change in $\text{rms}(P^* - E^*)$, as in Fig. 2, is shown for reference.

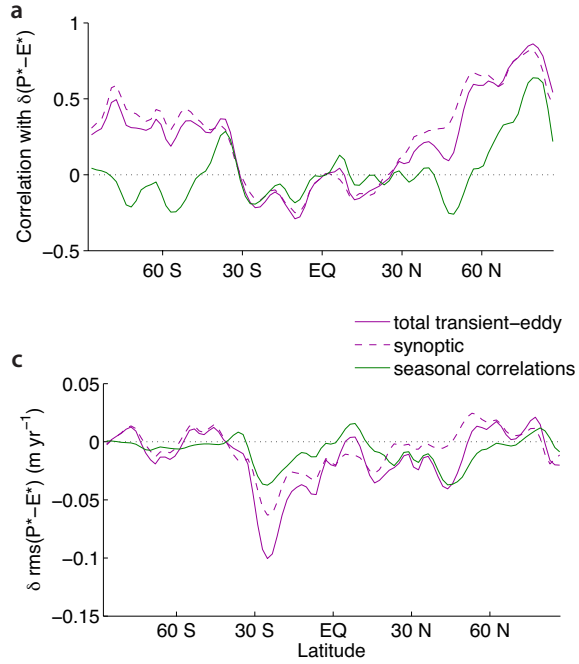


Figure S3. Decomposition of the transient-eddy term into synoptic (departures from monthly-mean) and seasonal-correlation components. a) As in Fig. 1g. b) As in Fig. 3c. GISS-E2-H is excluded from the analysis for this figure because the differing grids for thermodynamic and dynamic variables would require interpolation at every time step.

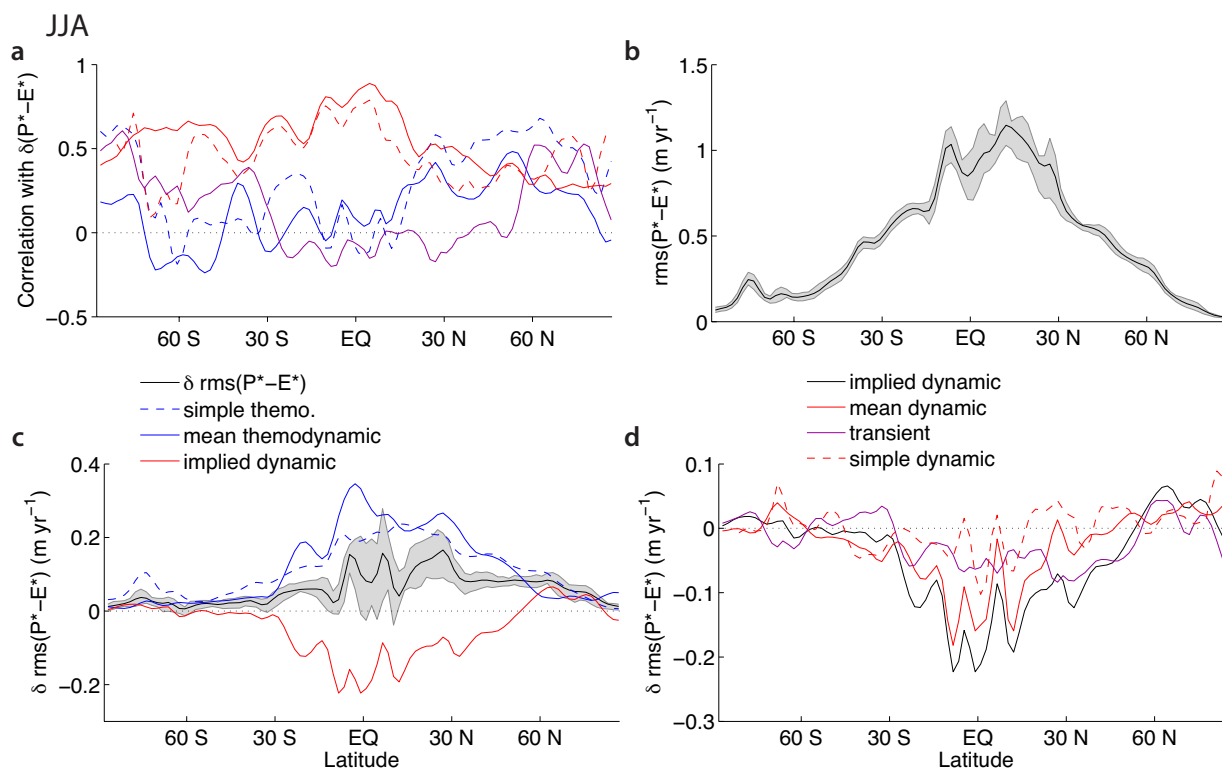


Figure S4. Key results reproduced for an analysis of the change in JJA $P^* - E^*$ climatology.

a) As in Fig. 1g. b) As in Fig. 2a. c) As in Fig. 2c. d) As in Fig. 3c.

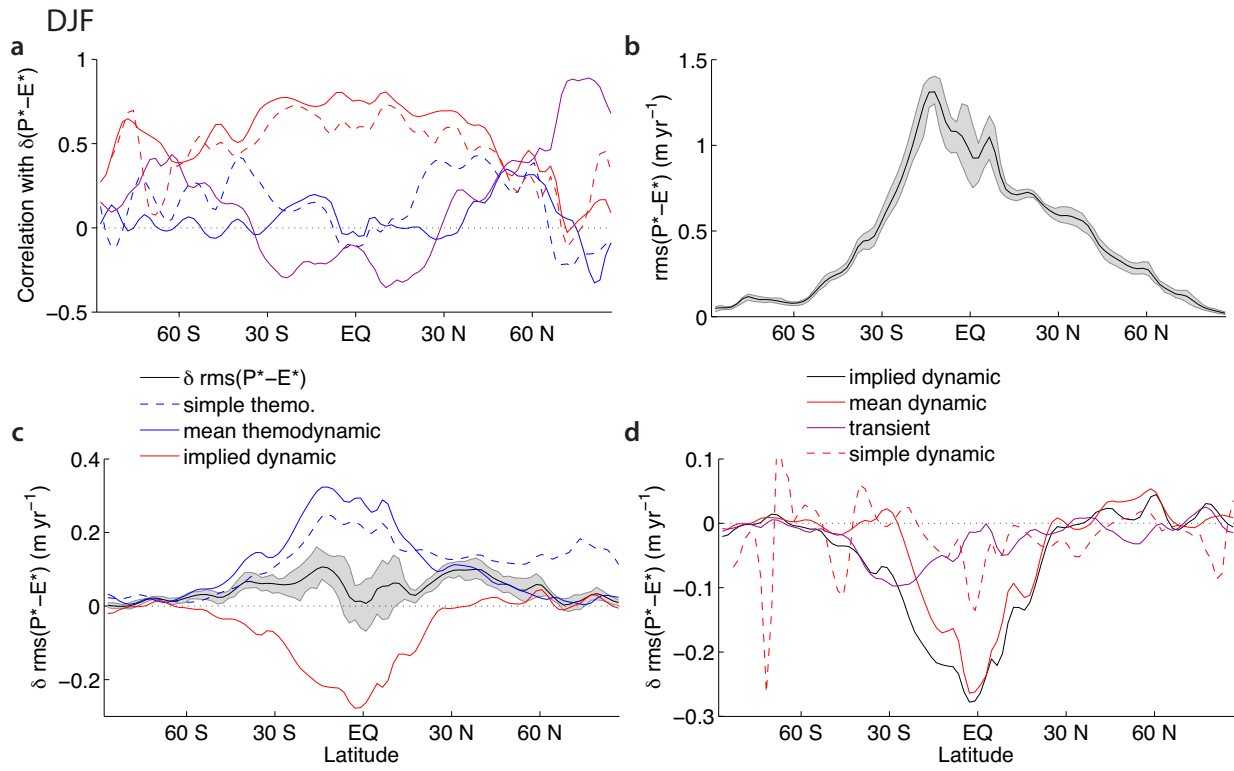


Figure S5. Key results reproduced for an analysis of the change in DJF $P^* - E^*$ climatology.

a) As in Fig. 1g. b) As in Fig. 2a. c) As in Fig. 2c. d) As in Fig. 3c.

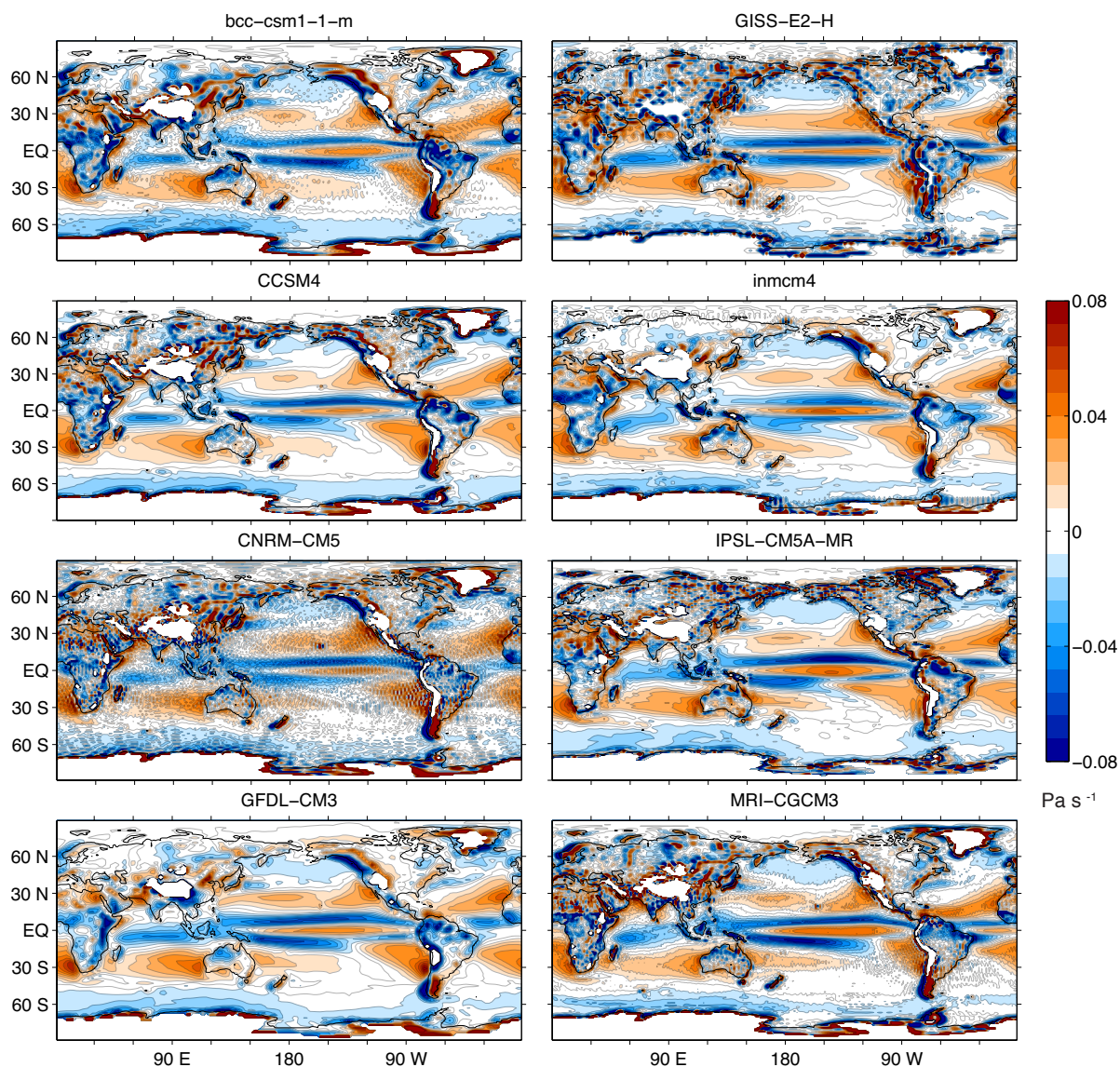


Figure S6. Raw unsmoothed 30-year average ω_{850} for the *PAST* (1976-2005) climate from selected CMIP5 models. The grid-scale noise evident in these fields is the motivation for the smoothing used in computing fields throughout this paper.